Electronic Supplementary Information

Synergetic effect of C and Ni on hydrogen release from Mg-Ni-electrochemically

synthesized reduced graphene oxide based hydride

Srikanta Panda, Marla V V Satya Aditya, and Sankara Sarma V Tatiparti*

Department of Energy Science & Engineering, Indian Institute of Technology Bombay,

Mumbai 400076, India

*Corresponding author E-mail: sankara@iitb.ac.in

S1. Hydrogen uptake

Prior to H release, ball milled nanocomposites were hydrogenated at ~15 bar and ~320 ℃ till saturation shown in Fig. S1. From these H uptake curves, it is observed that nanocomposites containing rGO showed lower incubation times. This suggests that rGO acts as a good catalyst during H uptake. Therefore, simultaneous addition of Ni and rGO reduces the incubation time during H uptake.
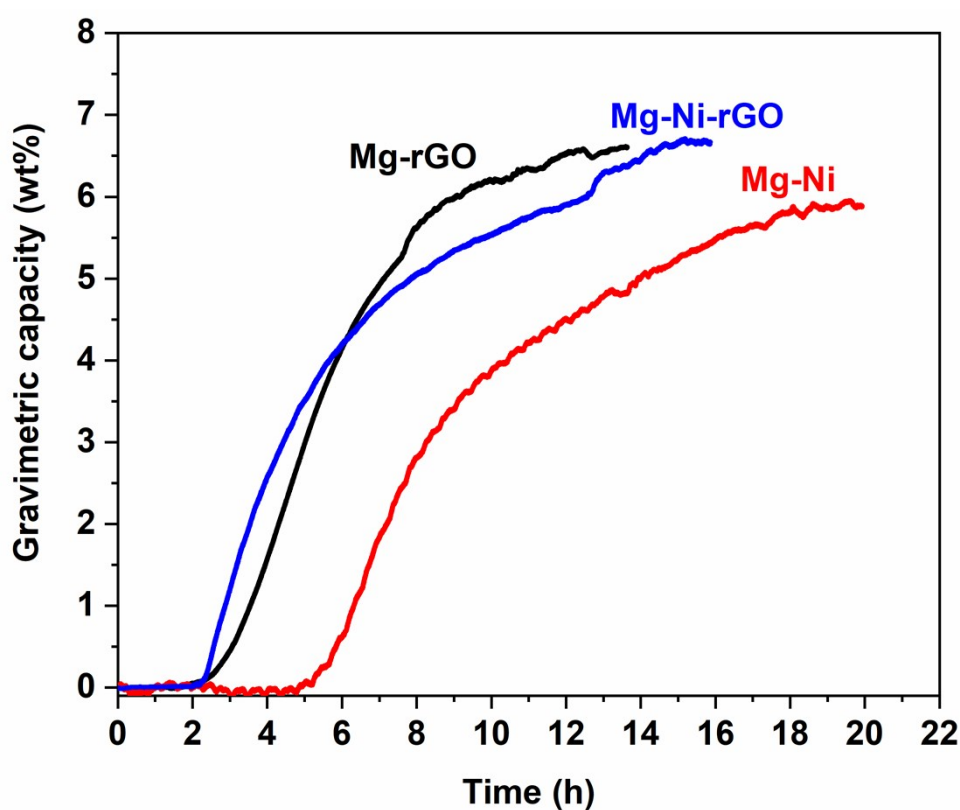

Fig. S1 H uptake in Mg-rGO, Mg-Ni and Mg-Ni-rGO nanocomposites at ~15 bar, ~320 ℃.

S2. Phase analysis

XRD patterns are obtained from all the nanocomposites after ball milling (BM), hydrogenated (Hyd), dehydrogenated (Dehyd) conditions to estimate the various phases as shown in Fig. S2. All the peaks in XRD were indexed using ICSD data base.[1] In all ball

milled nanocomposites (BM), Mg is the major phase (ICSD-642655) (Fig. S2). Also, a small peak at ~42.8˚ is observed that corresponds to MgO (ICSD-9863) phase. In ball milled Mg-Ni and Mg-Ni-rGO, a peak corresponding to Mg_2Ni is also observed at ~44.6˚ (Fig. S2b, c). Upon H uptake (hyd) Mg converts to MgH_2 (Fig. S2a-c, Hyd). Along with the MgH_2 phase, an additional intermediate hydride phase of Mg_2Ni (i.e. Mg_2NiH_x) is seen in Ni containing samples as a result of partial H uptake by Mg_2Ni (Fig. S2b and c, Hyd).
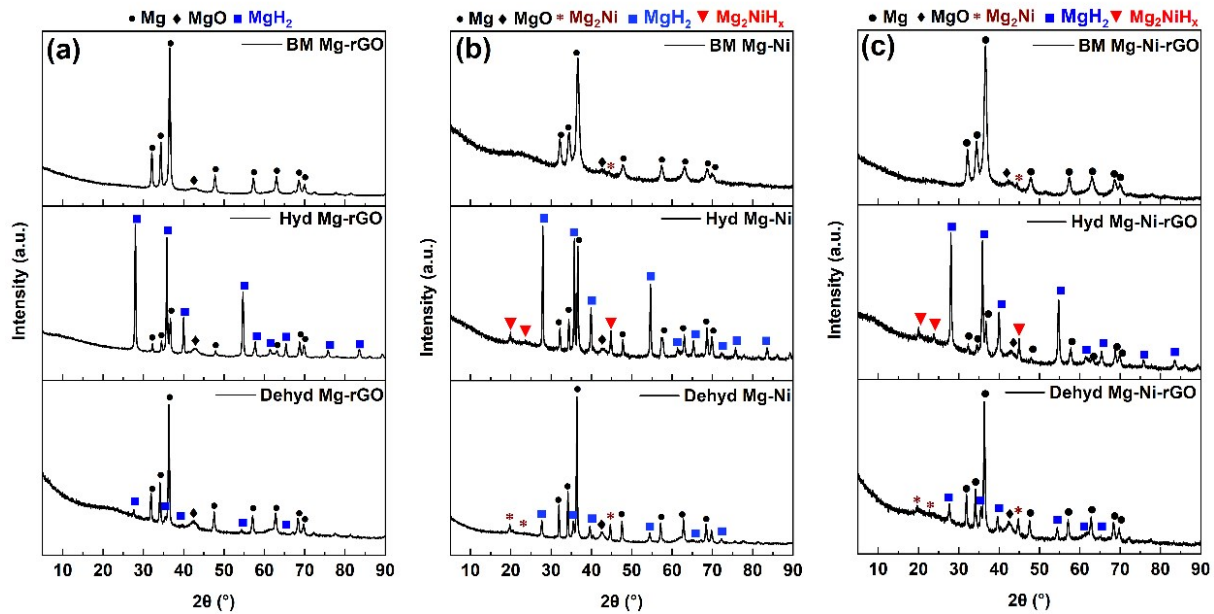

Fig. S2 XRD acquired after Ball milling (BM), H uptake (Hyd), H release (Dehyd) in (a) Mg-rGO, (b) Mg-Ni, (c) Mg-Ni-rGO.

S3. Rietveld refinement

To obtain the crystallographic information Rietveld refinement is performed on the data obtained from XRD. Refinement is performed using widely used FullProf software (version: 7.20).[2] Rietveld refinement of XRD obtained from hydrogenated (Hyd) Mg-rGO, Mg-Ni, Mg-Ni-rGO nanocomposites are shown in Fig. S3. Initially, the background of obtained XRD pattern is fitted with fifth order polynomial. Then scale factor, unit cell parameters, FWHM,

shape parameters and atom positions were refined subsequently. The observed (Y_{obs}) and calculated (Y_{calc}) pattern, residual ($Y_{obs}-Y_{calc}$), Bragg position and goodness of fit (χ^2) are shown in Fig. S3. The corresponding phase fractions are compiled in Table S1.
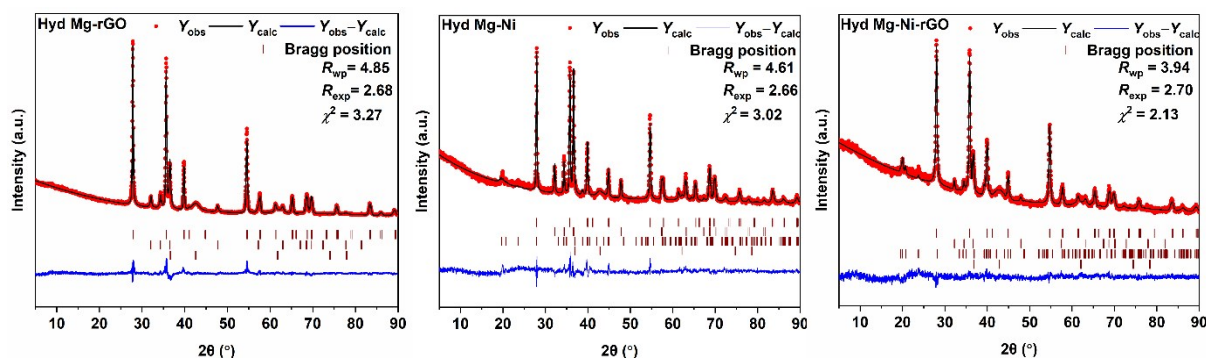

Fig. S3 Rietveld refinement of hydrogenated Mg-rGO (left), Mg-Ni (center), Mg-Ni-rGO (right) nanocomposites.

Table S1. Phase percentages estimated from Rietveld refinement in Mg-rGO, Mg-Ni, Mg-Ni-rGO upon H uptake.

	MgH$_2$ (%)	Mg (%)	Mg$_2$NiH$_x$ (%)	MgO (%)
Mg-rGO	58	20	-	22
Mg-Ni	63	11	24	2
Mg-Ni-rGO	75	10	13	2

S4. Deconvolution of core level O1s spectra

The core level O1s XPS spectra for Mg-rGO and Mg-Ni-rGO was obtained under Ball milled (BM), Hydrogenated (Hyd) and dehydrogenated (Dehyd) conditions. The XPS peaks were deconvoluted using Gaussian function[3] as shown in Fig. S4. The deconvoluted peaks at ~ 531.6-532.2 eV, ~ 533.5eV, ~ 534.3 eV were assigned to C=O,[4,5] MgO,[6] C-OH,[7,8] respectively. A new peak is observed in Mg-Ni-rGO nanocomposite in BM condition (Fig. S4b) at ~531.01 eV that corresponds to Ni-O-C interaction.[4] However, this peak is largely diminished after H uptake (Hyd) (Fig. S4b).
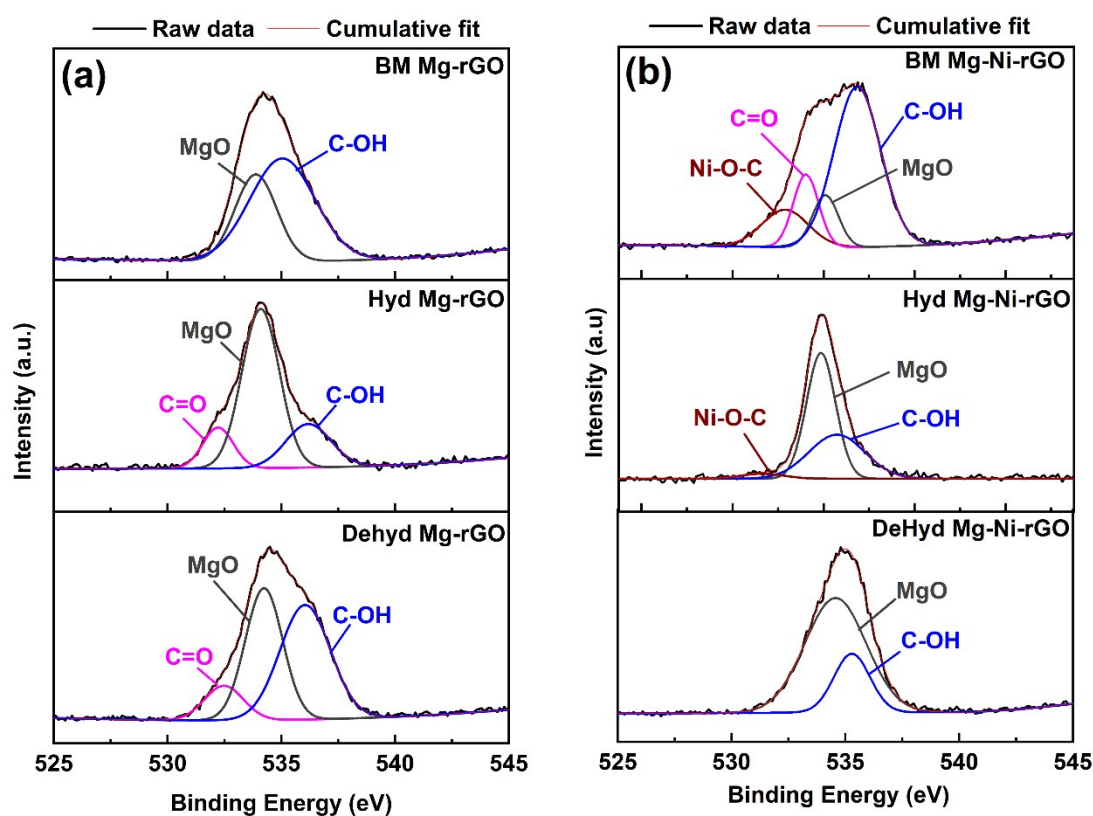

Fig. S4 Deconvoluted O1s core level XPS spectra after ball milling (BM), H uptake (Hyd), and H release (Dehyd) of (a) Mg-rGO, (b) Mg-Ni-rGO nanocomposites.

S5. Raman spectrum of electrochemically synthesized rGO

The Raman spectrum of electrochemically synthesized rGO is shown in Fig. S5. The D band and G band are observed at ~1350 cm^{-1} and ~1588 cm^{-1} respectively. The I_D/I_G ratio was estimated as 0.844.
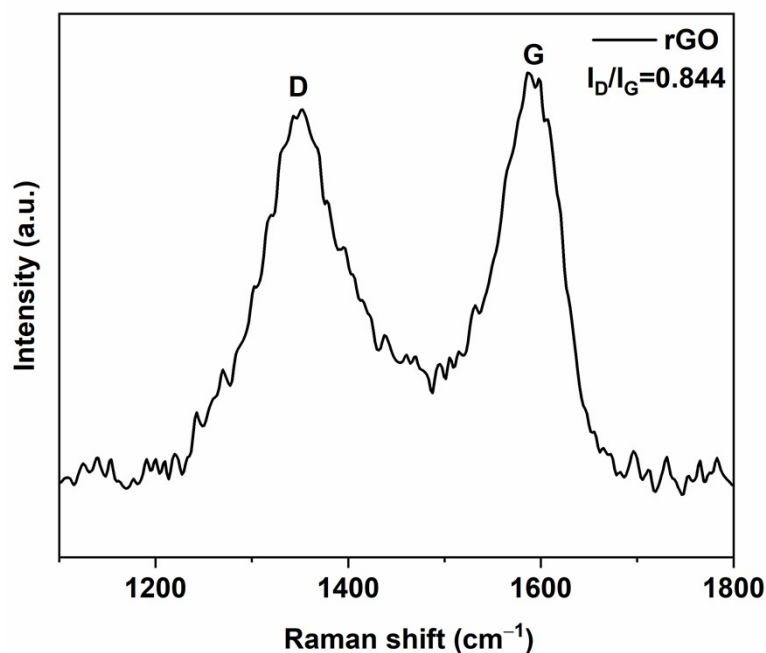

Fig. S5 Raman spectrum of electrochemically synthesised rGO.

S6. Estimation of activation energy (E_a) by Kissinger analysis

The activation energy (E_a) of all the catalyzed MgH_2 phases in Mg-Ni-rGO samples are estimated using Kissinger equation (eqn S1). Differential scanning calorimetry (DSC) was performed on hydrogenated Mg-Ni-rGO sample at the heating rates 3, 5, 7, 10 °C min^{-1}. Each of these profiles obtained from DSC were deconvoluted into four peaks corresponding to Ni-C, (Mg_2NiH_x)-C, Mg_2NiH_x and Mg-C catalyzed MgH_2 phase. For each catalyzed phase, the peak temperature at every heating rate is used in the Kissinger equation (eqn S1) to estimate respective E_a values. The linear fittings of the Kissinger equation for all the catalyzed phases are shown in Fig. S6.

$$\ln(\beta/T_p{}^2) = A - (E_a/RT_p) \qquad (S1)$$

where, β = heating rate (°C min^{-1}), T_p = peak temperature (K), E_a = activation energy (kJ mol^{-1} H), R = gas constant (8.314 J mol^{-1} K^{-1}), A = constant.
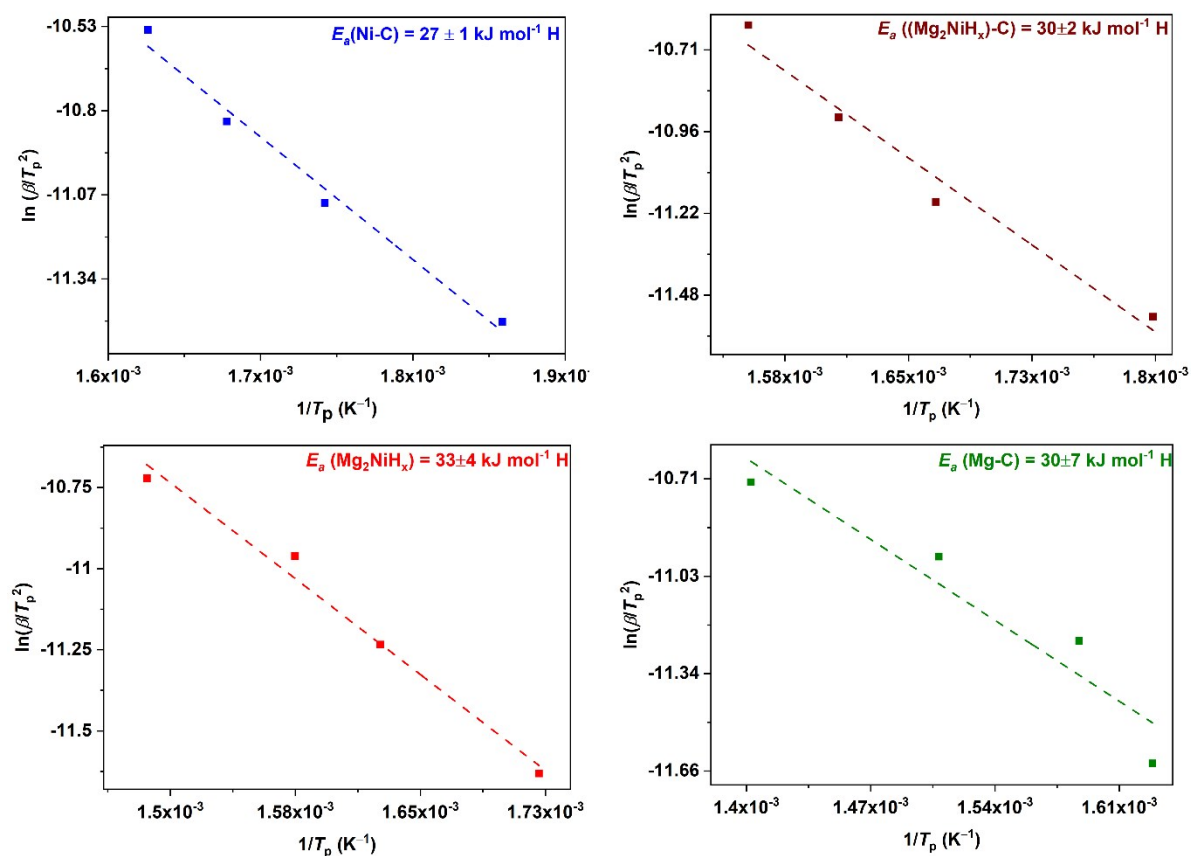

Fig. S6 Estimation of activation energy for each catalysed MgH$_2$ using Kissinger analysis.

References

1   ICSD:, https://icsd.fiz-karlsruhe.de/, (accessed 25 December 2020).

2   J. Rodriguez-Carvajal, FULLPROF: a Program for Rietveld Refinement and Pattern Matching Analysis, *Abstracts of the Meeting on Powder Diffraction*, Toulouse, France, 1990.

3   G. H. Major, N. Fairley, P. M. A. Sherwood, M. R. Linford, J. Terry, V. Fernandez

and K. Artyushkova, Practical guide for curve fitting in x-ray photoelectron spectroscopy, *J. Vac. Sci. Technol. A*, 2020, **38**, 061203.

4   Z. Wu, X. L. Huang, Z. L. Wang, J. J. Xu, H. G. Wang and X. B. Zhang, Electrostatic induced stretch growth of homogeneous β-Ni(OH)$_2$ on graphene with enhanced high-rate cycling for supercapacitors, *Sci. Rep.*, 2014, **4**, 1–8.

5   H. Lee, J. S. Kim, K. Y. Lee, K. H. Park and J. Bae, Elucidation of an intrinsic parameter for evaluating the electrical quality of graphene flakes, *Sci. Rep.*, 2019, 1–8.

6   S. Sugiyama, T. Miyamoto, H. Hayashi and J. B. Moffat, Oxidative Coupling of Methane on MgO-MgSO$_4$ Catalysts in the Presence and Absence of Carbon Tetrachloride, *Bull. Chem. Soc. Jpn.*, 1996, **69**, 235–240.

7   K. Garg, R. Shanmugam and P. C. Ramamurthy, Synthesis , characterisation and optical studies of new tetraethyl- rubyrin-graphene oxide covalent adducts, *Opt. Mater. (Amst).*, 2018, **76**, 42–47.

8   D. Yang, A. Velamakanni, G. Bozoklu, S. Park, M. Stoller, R. D. Piner, S. Stankovich, I. Jung, D. A. Field, C. A. Ventrice and R. S. Ruoff, Chemical analysis of graphene oxide films after heat and chemical treatments by X-ray photoelectron and Micro-Raman spectroscopy, *Carbon*, 2009, **47**, 145–152.